Electronic Supplementary Material (ESI) for Journal of Materials Chemistry C

Confined organization of fullerene units along high polymer chains

Lei Fang,[†] Peng Liu,[‡] Benjamin R. Sveinbjornsson,[§] Sule Atahan-Evrenk,[¶] Koen Vandewal,[⊥] Sílvia Osuna,[‡] Gonzalo Jiménez-Osés,[‡] Supriya Shrestha,[¶] Gaurav Giri,[†] Peng Wei,[†] Alberto Salleo,[⊥] Alán Aspuru-Guzik,[¶] Robert H. Grubbs,[§] K. N. Houk,[‡] and Zhenan Bao[†]*

[†] *Department of Chemical Engineering, Stanford University, Stanford, CA 94305, United States, Email: zbao@stanford.edu*

[‡] *Department of Chemistry and Biochemistry, University of California, Los Angeles, CA 90095, United States*

[§] *Division of Chemistry and Chemical Engineering, California Institute of Technology, Pasadena, CA 91125, United States*

[¶] *Department of Chemistry & Chemical Biology, Harvard University, Cambridge, MA 02138*

[⊥] *Department of Materials Science and Engineering, Stanford University, Stanford, CA 94305, United States*

Supporting Information

1. Molecular Dynamics Simulations

Substrate parameters for the MD simulations were generated within the ANTECHAMBER module of AMBER 11[1] using the general AMBER force field (GAFF),[2] with partial charges set to fit the electrostatic potential generated at the HF/6-31G(d) level by the RESP model.[3] The charges were calculated according to the Merz-Singh-Kollman scheme[4, 5] using Gaussian 09.[6] Since it is not practical to compute the HF

electrostatic potential (ESP) for the polymer, the HF/6-31G(d) RESP partial charges were obtained by fitting with the monomer unit. Each polymer unit is immersed in a pre-equilibrated truncated octahedral box of toluene molecules[7] with an internal offset distance of 10 Å, using the LEAP module.[8] This resulted in the addition of around 2,500 solvent molecules. All systems were neutral, and no explicit counterions were added. A two-stage geometry optimization approach was performed. First, a short minimization of the toluene molecules positions, with positional restraints on solute by a harmonic potential with a force constant of 500 kcal mol^{-1} $Å^{-2}$ was done. The second stage was an unrestrained minimization of all the atoms in the simulation cell. Then, the systems were gently heated using six 50 ps steps, incrementing the temperature 50 K each step (0-300 K) under constant-volume, periodic-boundary conditions and the particle-mesh Ewald approach[9] to introduce long range electrostatic effects. For these steps, an 8 Å cutoff was applied to Lennard-Jones and electrostatic interactions. Bonds involving hydrogen were constrained with the SHAKE algorithm.[10] Harmonic restraints of 10 kcal mol^{-1} were applied to the solute, and the Langevin equilibration scheme is used to control and equalize the temperature.[11] The time step was kept at 1 fs during the heating stages, allowing potential inhomogeneities to self-adjust. Each system is then equilibrated for 2 ns with a 2 fs time step at a constant pressure of 1 atm. Finally, a 20 ns unrestrained MD trajectory at constant pressure (1 atm) and temperature (300 K) was collected and analyzed using the PTRAJ module in AMBER.[1]

The starting structure was constructed with a *trans*-isotactic backbone with 10 repeating monomers for each polymer, five on each side of the backbone. The distance between the

centers of adjacent C_{60} is 9.54 Å (with the surface-surface distance 2.4 Å) in the starting geometry. (Figure S1).

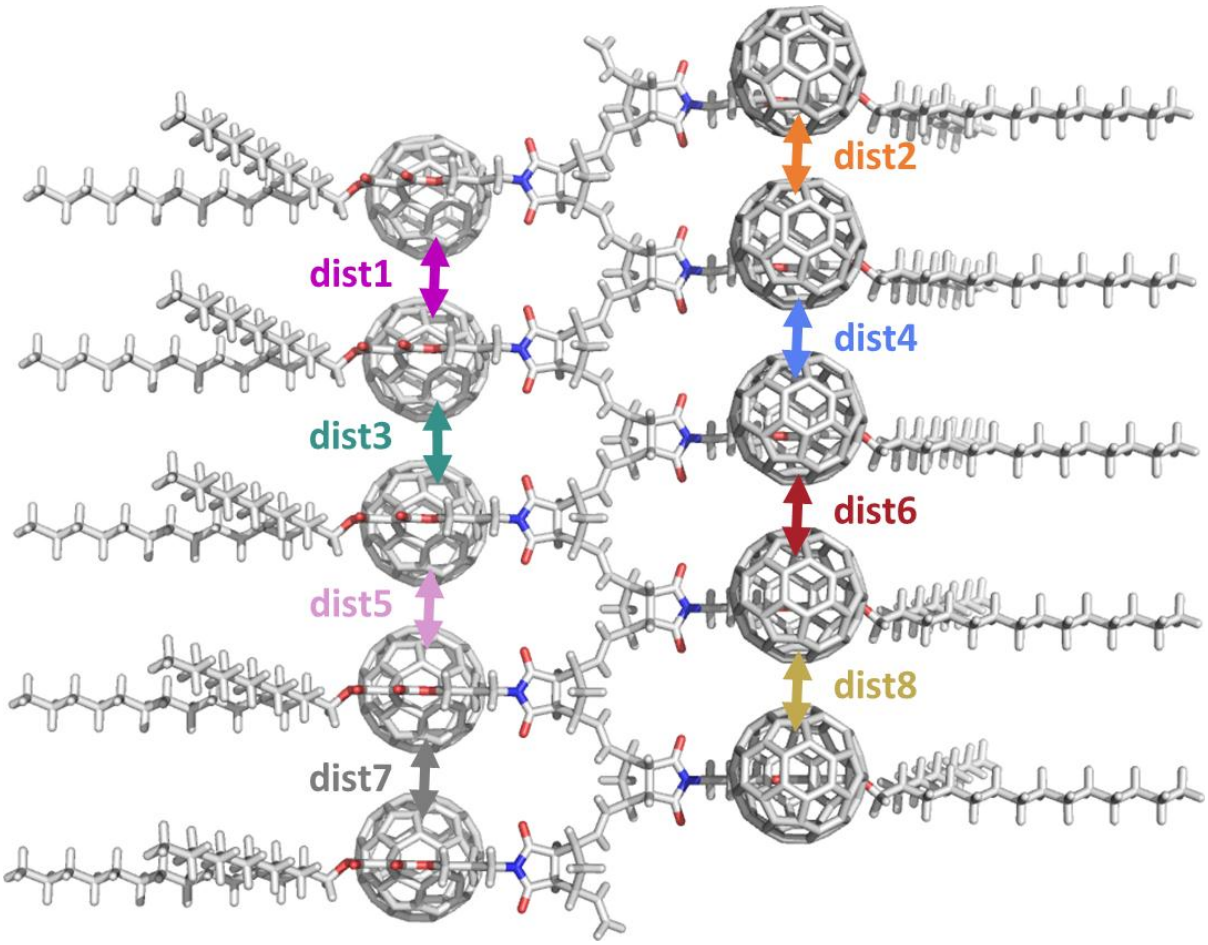

Figure **S1**. Initial structure of polymer **4d** (m=3) in the molecular dynamics simulation. The distances between the centers of the C_{60} groups are labeled with the same color code as in the histogram in Figure 2.

To quantify the difference of flexibility of the backbone and the sidechain C_{60} groups, the atomic positional fluctuations for the inner fullerene centroids and the polymer backbone (succinimide nitrogen atoms) were calculated as B-factors ($Å^2 \times \frac{8}{3}\pi^2$) and mass-weighted

averaged along the MD trajectories[12, 13] (Table S1). Rotation and translation were suppressed by performing a previous RMS fit to the first simulation snapshot. For all polymers, the B-factors of the C_{60} groups are significantly larger than those of the backbone. This indicates the backbone is much more rigid than the sidechains. In agreement with the trend of the inter-C_{60} distances reported in the manuscript, the C_{60} units in polymer **4f** (*m* = 12) are also much more flexible than those in **4e** (*m* = 6) and **4d** (*m* = 3).

Table S1. Computed B-factors of the centers of C60 units and the succinimide nitrogen atoms on the backbone for polymers **4d**, **4e**, and **4f**.

Polymer	B-factor C_{60}	B-factor backbone
4d (*m* = 3)	421.98	40.07
4e (*m* = 6)	618.38	59.49
4f (*m* = 12)	1428.65	174.5

2. Quantum Chemistry Calculations

Based on the 20 ns trajectories obtained by molecular dynamics calculations, we have extracted 100 groups of two adjacent C_{60} units for every snapshot every 200 fs, in order to compare the magnitude of the transfer integrals for polymer **4d** (*m* = 3) and **4f** (*m* = 12). The transfer integrals for the LUMO orbitals were calculated within the dimer approximation[14, 15] at the B3LYP/6-31G(d)[16-20] level of theory as implemented in Q-Chem 3.2 quantum chemistry package.[21] Although the 6-31G(d) basis is known to underestimate[22] the strength of the couplings, it has been shown[23] that qualitatively correct results were obtained at this level of theory. The solubilizing 2-decyltetradecyl

group and the spacers to the polymer backbone are replaced by -*methyl* groups to reduce the size of the system. Figure S2 shows a typical structure used in the transfer integral calculation.

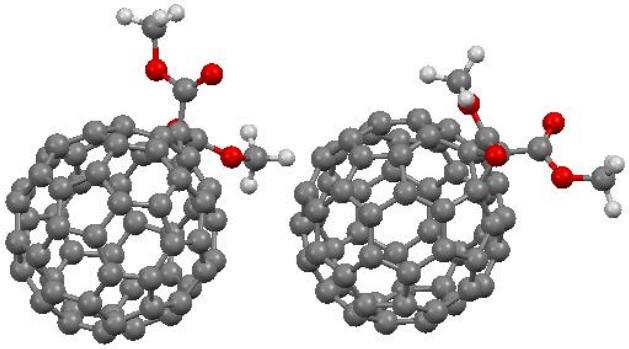

Figure S2. A typical dimer of C_{60} derivatives used in the transfer integral calculation. The solubilizing groups and the spacers to the polymer backbone are replaced by *methyl* groups for simplification.

3. Synthetic procedures

General procedures

All reagents and starting materials were purchased from commercial sources and used without further purification, unless otherwise noted. ^{1}H and ^{13}C NMR spectra were recorded using Varian Inova 500 or Inova 400 in deuterated solvents at 293 K. Mass spectrograms were recorded on either a Finnigan MAT95Q Hybrid Sector (EI, HRMS) or a Bruker Reflex II (MALDI-TOF) mass spectrometer operated in linear mode with delayed Extraction. Size exclusion chromatography (SEC) was performed in THF solution and the molecular weights calculated using a calibration curve based on polystyrene standards. Thermal gravimetric analyses (TGA) were performed using a

Mettler TOLEDO TGA/SDTA 851e at a heating rate of 10 °C/min under a nitrogen flow (20 mL/min).

Synthesis and Characterization of 2a~d and 2f

A solution of *cis*-5-norbornene-*exo*-2,3-dicarboxylic anhydride (1.5 mmol), the corresponding *α,ϖ*-amino alcohol, and catalytic amount of triethyl amine (25 μL) in toluene (15 mL) was refluxed with a Dean-Stark trap under argon for 4 h. The Dean-Strak trap is then removed and Meldrum's acid (1.8 mmol) was added to the reaction mixture. After another 12 h of reflux, the reaction was allowed to cool down to RT before the solvent was removed under reduced pressure. The residue was purified by column chromatography (SiO_2, CH_2Cl_2 - ethyl acetate - ethyl acetate/MeOH = 5:1) to give the malonic acids as sticky colorless oil. The intermediate was then mixed with the hydroxyl functionalized solubilizing agents (1 mmol), and a catalytic amount of 4-dimethlyaminopyridine in dry CH_2Cl_2 (5 mL). After the addition of 1 M solution of *N,N'*-dicyclohexylcarbodiimide in CH_2Cl_2 (1.2 mmol, 1.2 mL), the solution turned cloudy in a few minutes. The reaction mixture was stirred at RT for 12 h before the solvent was removed under reduced pressure. The residue was purified by column chromatography (SiO_2, ethyl acetate/hexane = 1:2) to give the product as white foam (**2a~c**) or sticky oil (**2d**).

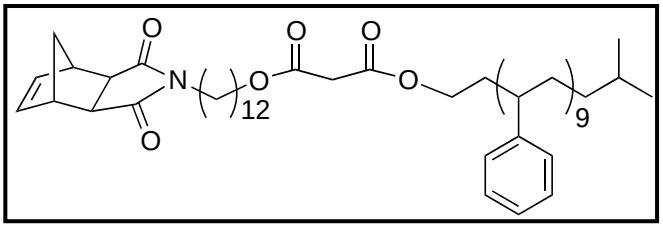

2a ^{1}H NMR (500 MHz, $CDCl_3$, 298 K) δ = 0.56-0.71 (m, 6H), 0.83-2.47 (m, 54H), 2.63 (s, 2H), 3.14-3.20 (m, 2H), 3.25 (s, 2H), 3.44 (t, 2H, *J* = 7.5 Hz), 3.77 (br, 2H), 4.04-4.08

(m, 2H), 6.23 (s, 2H), 6.53-7.18 (m, 45 H). ^{13}C NMR (125 MHz, $CDCl_3$, 298 K) δ = 11.1, 25.6, 26.8, 27.6, 28.9, 29.0, 29.1, 29.3, 31.4, 38.6, 40.4, 41.2, 42.3, 45.0, 47.6, 63.6, 65.4, 125.4 (br), 127.4-128.4 (m, br), 137.7, 145.2-145.5 (m), 166.3, 166.4, 177.9. MALDI MS: [$C_{30}H_{47}NO_6(C_8H_8)n$ + H^+] *m/z* = 934.6021 (*n*=4); 1038.6658 (*n*=5); 1142.7283 (*n*=6); 1246.7905 (*n*=7); 1350.8527 (*n*=8); 1454.9139 (*n*=9); 1558.9756 (*n*=10); 1663.0358 (*n*=11).

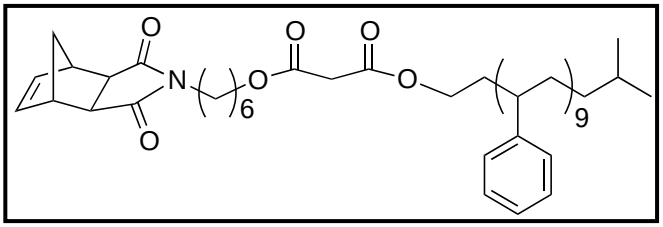

2b: ^{1}H NMR (400 MHz, $CDCl_3$, 298 K) δ = 0.56-0.72 (m, 6H), 0.88-2.36 (m, 42H), 2.67 (s, 2H), 3.16-3.21 (m, 2H), 3.27 (s, 2H), 3,45 (t, 2H, *J* = 7.2 Hz), 3,78 (br, 2H), 4.05-4.08 (m, 2H), 6.28 (s, 2H), 6.53-7.14 (m, 45 H). ^{13}C NMR (125 MHz, $CDCl_3$, 298 K) δ = 11.1, 25.8, 27.7, 29.1, 29.3, 31.3, 33.8, 35.2, 40.4, 41.3, 45.0, 47.8, 63.1, 64.2, 125.5 (br), 127.5-128.0 (m), 137.7, 145.3, 166.2, 166.4, 177.9. MALDI MS: [$C_{24}H_{35}NO_6(C_8H_8)n$ + Na^+] *m/z* = 976.5492(*n*=5); 1080.6116 (*n*=6); 1184.6717 (*n*=7); 1288.7411 (*n*=8); 1392.8079 (*n*=9); 1496.8614 (*n*=10); 1600.9225 (*n*=11); 1704.9945 (*n*=12).

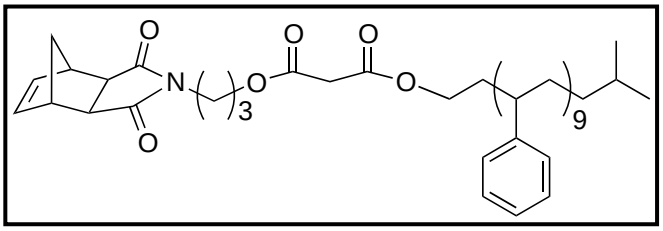

2c: ^{1}H NMR (500 MHz, $CDCl_3$, 298 K) δ = 0.56-0.72 (m, 6H), 0.84-2.34 (m, 36H), 2.65 (s, 2H), 3.17-3.22 (m, 2H), 3.25 (s, 2H), 3.52 (t, 2H, *J* = 6.5Hz), 3.78-3.90 (m, 2H), 4.05-4.12 (m, 2H), 6.25 (s, 2H), 6.52-7.21 (m, 45H). ^{13}C NMR (125 MHz, $CDCl_3$, 298 K) δ = 11.0, 26.7, 31.4, 33.9, 35.4, 40.4, 41.1, 45.1, 47.7, 62.6, 63.8, 125.5-126.2 (m), 127.6-

128.5 (m), 137.7, 145.2, 166.1, 166.3, 177.8. MALDI MS: [$C_{21}H_{29}NO_6(C_8H_8)n + Na^+$] *m/z* = 1038.5611 (*n*=6); 1142.6302 (*n*=7); 1246.6925 (*n*=8); 1350.7570 (*n*=9); 1454.8155 (*n*=10); 1558.8794 (*n*=11).

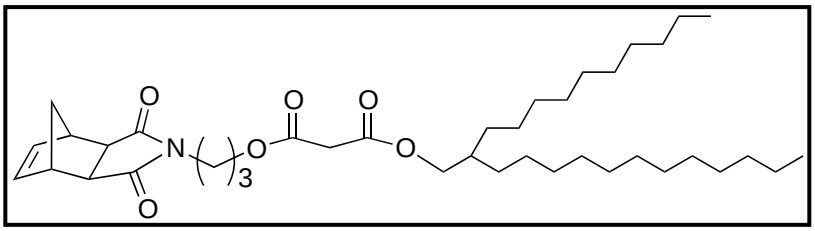

2d: ^{1}H NMR (500 MHz, $CDCl_3$, 298 K) δ = 0.88 (t, 6H, *J* = 6.5 Hz), 1.19-1.31 (m, 41H), 1.51-1.53 (m, 1H), 1.62 (br, 1H), 1.94 (m, 2H), 2.69 (s, 2H), 3.28 (s, 2H), 3.39 (s, 2H), 3.57 (t, 2H, *J* = 7.0Hz), 4.04 (d, 2H, *J* = 5.5Hz), 4.14 (t, 2H, *J* = 6Hz), 6.29 (s, 2H). ^{13}C NMR (125 MHz, $CDCl_3$, 298 K) δ = 13.9, 22.5, 26.4, 26.6, 26.7, 29.1, 29.4, 29.5, 29.7, 29.9, 30.7, 30.8, 31.7, 35.2, 36.9, 41.2, 42.5, 44.9, 47.6, 62.4, 65.2, 68.0, 137.5, 166.1, 166.3, 177.5. MALDI MS: [$C_{39}H_{65}NO_6$] *m/z* = 644.4869 ($M+H^+$); 666.4520 ($M+Na^+$).

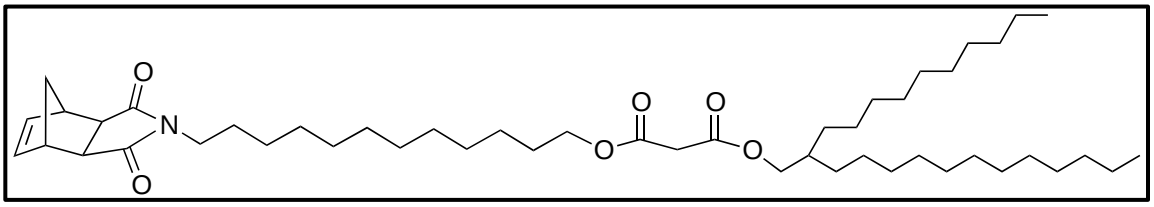

2f: ^{1}H NMR (500 MHz, $CDCl_3$, 298 K) δ = 0.85 (t, 6H, *J* = 6.5 Hz), 1.20-1.32 (m, 57H), 1.47-1.51 (m, 3H), 1.60-1.63 (m, 3H), 2.65 (s, 2H), 3.25 (s, 2H), 3.35 (s, 2H), 3.43 (t, 2H, *J* = 7.5 Hz), 4.02 (d, 2H, *J* = 5.5 Hz), 4.01 (t, 2H, *J* = 6.5 Hz), 6.26 (s, 2H). ^{13}C NMR (125 MHz, $CDCl_3$, 298 K) δ = 14.1, 22.6, 25.7, 26.6, 26.9, 27.7, 28.4, 29.1, 29.2, 29.3, 29.4, 29.5, 29.6, 29.9, 31.0, 31.9, 37.1, 38.7, 41.6, 42.6, 45.1, 47.7, 65.6, 68.2, 137.8, 166.6, 166.7, 178.0. MALDI-MS: [$C_{48}H_{83}NO_6$] *m/z* = 792.6132 ($M+Na^+$).

Synthesis and Characterization of 3a~d and 3f

C_{60} (0.18 mmol) was fully dissolved in dry toluene (100 mL) before **2a~d** (0.12 mmol) and carbontetrabromide (0.14 mmol) was added into the solution. A solution of DBU (0.14 mmol) in toluene (20 mL) was then added to the reaction mixture dropwise over 6 h at RT. After stirring further for 24 h, the solution turned from purple into brown. Solvent was removed under reduced pressure and the residue was purified by column chromatography (SiO_2, CH_2Cl_2) to give **3a~d** as red foams. The products were further purified by preparative recycling GPC (eluent: $CHCl_3$) for the polymerization.

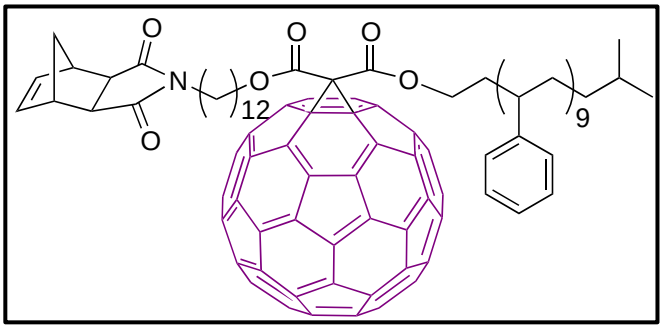

3a: ^{1}H NMR (500 MHz, $CDCl_3$, 298 K) δ = 0.55-0.71 (m, 6H), 0.89-2.40 (m, 54H), 2.67 (s, 2H), 3.27 (s, 2H), 3.45 (t, 2H, J = 7.5 Hz), 4.05-4.41 (m, 4H), 6.28 (s, 2H), 6.53-7.18 (m, 45H). ^{13}C NMR (125 MHz, $CDCl_3$, 298 K) δ = 11.1, 21.4, 25.9, 26.9, 27.7, 28.5, 29.1, 29.4, 29.5, 29.7, 31.4, 38.7, 40.5, 42.7, 45.1, 47.7, 65.6, 67.3, 71.5, 125.2, 125.6 (br), 127.6-128.6 (m), 129.0, 137.8, 138.8, 139.0, 140.8, 140.9, 141.8, 142.1, 142.9, 143.8, 144.5, 144.6, 145.1-145.3 (m), 163.5, 178.0. MALDI MS: $[C_{90}H_{45}NO_6(C_8H_8)n + H]^+$ *m/z* = 1652.5740 (*n*=4); 1756.6402 (*n*=5); 1860.7050 (*n*=6); 1964.7723 (*n*=7); 2068.8279 (*n*=8); 2172.8884 (*n*=9); 2276.9641 (*n*=10).

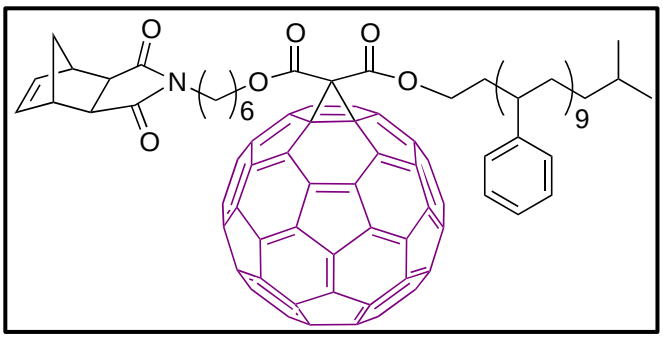

3b: ^{1}H NMR (500 MHz, $CDCl_3$, 298 K) δ = 0.55-0.71 (m, 6H), 0.84-2.35 (m, 42H), 2.67 (s, 2H), 3.27 (s, 2H), 3.44 (t, 2H, *J* = 7.5 Hz), 4.05-4.39 (m, 4H), 6.28 (s, 2H), 6.40-7.13 (m, 45H). ^{13}C NMR (125 MHz, $CDCl_3$, 298 K) δ = 10.5, 19.1, 25.5, 26.5, 27.7, 30.9, 38.5, 40.4(br), 42.4, 45.2, 47.8, 65.4, 67.2, 71.5, 125.6, 127.6-128.5(m), 137.8, 138.8, 139.0, 140.9, 141.8, 142.2, 142.9, 143.8, 144.6, 144.7, 144.9-145.2(m), 163.5, 178.0. MALDI-MS: $[C_{84}H_{33}NO_6(C_8H_8)n + Na]^+$ *m/z* = 1694.87 (*n*=5); 1798.83 (*n*=6); 1902.81 (*n*=7); 2006.77 (*n*=8); 2110.73 (*n*=9); 2214.71 (*n*=10); 2318.66 (*n*=11).

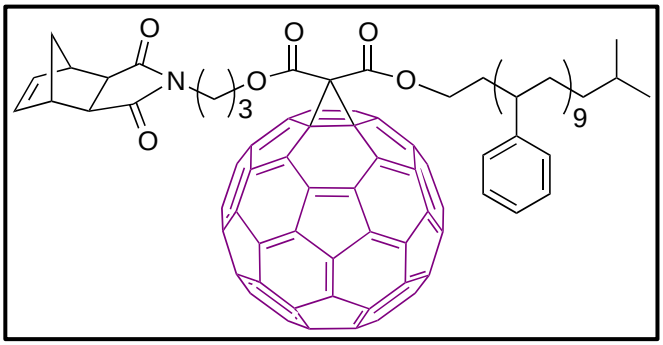

3c: ^{1}H NMR (500 MHz, $CDCl_3$, 298 K) δ = 0.54-0.71 (m, 6H), 0.90-2.32 (m, 36H), 2.70 (s, 2H), 3.27 (s, 2H), 3.54-3.61 (m, 2H), 4.07-4.42 (m, 4H), 6.27 (s, 2H), 6.51-7.24 (m, 45H). ^{13}C NMR (125 MHz, $CDCl_3$, 298 K) δ = 11.1, 27.0, 29.2, 30.8, 31.4, 32.4, 35.6, 36.7, 40.5, 42.8, 44.2, 45.2, 47.8, 63.3, 64.6, 125.6, 127.6-128.5 (m), 137.8, 138.7, 138.9, 140.9, 141.9, 142.2, 142.9, 143.8, 144.6, 144.8, 145.1-146.0 (m), 163.3, 177.8. MALDI-

MS: $[C_{81}H_{27}NO_6(C_8H_8)n + Na]^+$ *m/z* = 1652.5285 (*n*=5); 1756.5713 (*n*=6); 1860.6269 (*n*=7); 1964.6789 (*n*=8); 2068.7231 (*n*=9); 2172.7886 (*n*=10); 2276.8317 (*n*=11).

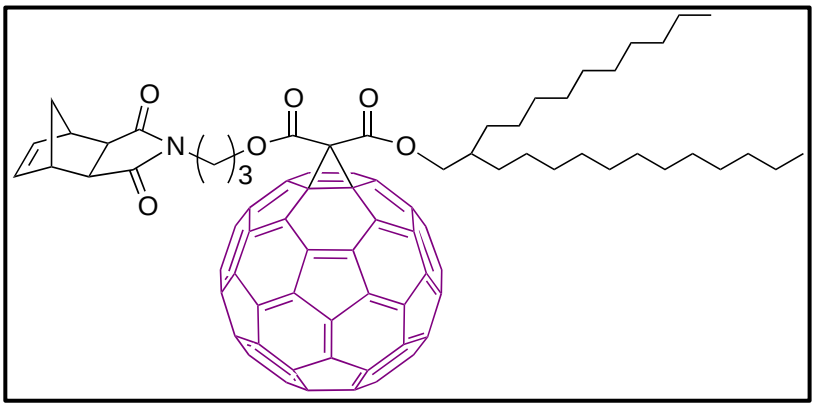

3d: ^{1}H NMR (500 MHz, $CDCl_3$, 298 K) δ = 0.87 (t, 6H, *J* = 6.5 Hz), 1.24-1.42, (m, 41H), 1.53-1.55 (m, 1H), 1.82-1.84 (m, 1H), 2.09-2.15 (m, 2H), 2.74 (s, 2H), 3.29 (s, 2H), 3.67 (t, 2H, *J* = 7.0 Hz), 4.43 (d, 2H, *J* = 5.5 Hz), 4.49 (t, 2H, *J* = 6 Hz), 6.29 (s, 2H). ^{13}C NMR (125 MHz, $CDCl_3$, 298 K) δ = 14.1, 22.7, 26.7, 27.1, 29.4, 29.6, 29.7, 30.1, 31.1, 31.9, 35.6, 37,4, 42.8, 45.2, 47.8, 52.3, 64.7, 70.1, 71.5, 137.8, 138.6, 139.2, 140.9, 141.9, 142.2, 142.9, 143.0, 143.8, 144.6, 144.8, 145.0, 145.1, 145.2, 145.4, 163.5, 177.8. MALDI MS: $[C_{99}H_{63}NO_6 + H]^+$ *m/z* = 1362.4712.

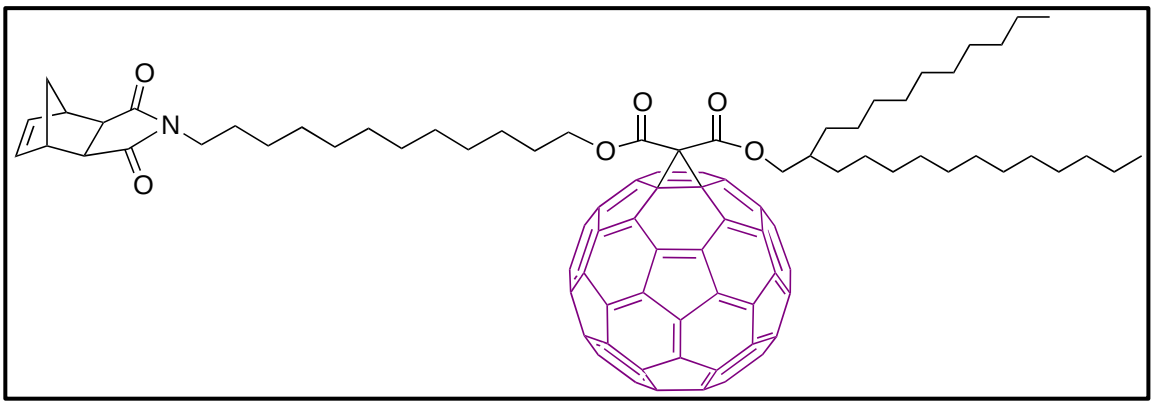

3f: ^{1}H NMR (500 MHz, $CDCl_3$, 298 K) δ = 0.87 (t, 6H, *J* = 6.5 Hz), 1.24-1.54 (m, 60H), 1.81-1.84 (m, 3H), 2.66 (s, 2H), 3.26 (s, 2H), 3.43 (t, 2H, *J* = 7.5 Hz), 4.39 (d, 2H, *J* = 5.0 Hz), 4.47 (t, 2H, *J* = 6.5 Hz), 6.27 (s, 2H). ^{13}C NMR (125 MHz, $CDCl_3$, 298 K) δ = 14.1,

22.7, 25.9, 26.8, 26.9, 27.7, 28.6, 29.1, 29.2, 29.3, 29.4, 29.5, 29.6, 29.7, 30.1, 30.9, 31.2, 31.9, 37.4, 38.7, 42.7, 45.1, 47.7, 67.4, 69.8, 71.7, 137.8, 138.8, 139.0, 140.9, 141.8, 142.1, 142.9, 143.0, 143.8, 144.5, 144.6, 144.8, 145.1-145.4 (m), 163.6, 163.8, 178.0. MALDI-MS: $[C_{108}H_{81}NO_6]$ *m/z* = 1488.6062 ($M+H^+$); 1510.5962 ($M+Na^+$).

Synthesis of 4a~d, f

In a glovebox, the [Ru] catalyst was dissolved in degassed toluene in a vial to make a catalyst stock solution (1 mg/mL). **3a~d** or **3f** was also dissolved in degassed toluene to make a reaction solution (30 mg/mL) in a vial with magnetic stirring bar. To the reaction solution was added the corresponding amount of catalyst solution while stirring. The reaction was allowed to proceed for 2 h before transferred out of the glovebox. The mixture was stirred open to the air for another 30 min and then sealed for storage.

4. Gel Permeation Chromatography

Analytical gel permeation chromatography (GPC) experiments were performed on a Malvern VE2001 GPC solvent/sample Module with three ViscoGEL^{TM} I-MBHMW-3078 columns. Refractive index detector and UV/vis absorption detector were employed to measure the concentration of the eluted solution. The flow rates were set to 1 mL/min while the temperature was kept at 25 °C. The column set was calibrated by the retention time of 12 mono-dispersed polystyrene standards with molecular weights ranging from 1.05 kDa to 3800 kDa. The molecular weights and PDI of the samples were calculated on the basis of the sample retention time and the aforementioned calibration curve. THF was used as the eluent for **4a~c** while chlorobenzene was used for **4d** and **4f**.

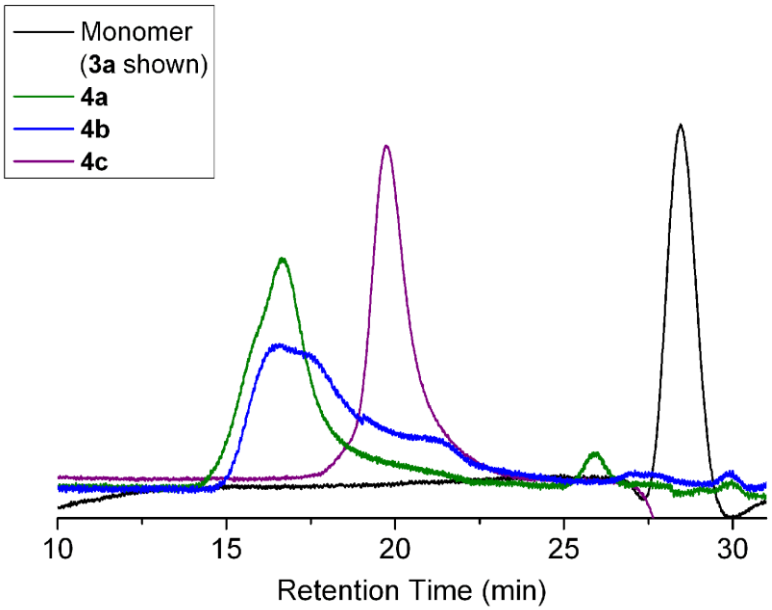

Figure S3: GPC chromatogram of polymers **4a**, **4b** and **4c**, compared to that of monomer **3a**, recorded using THF as the eluent.

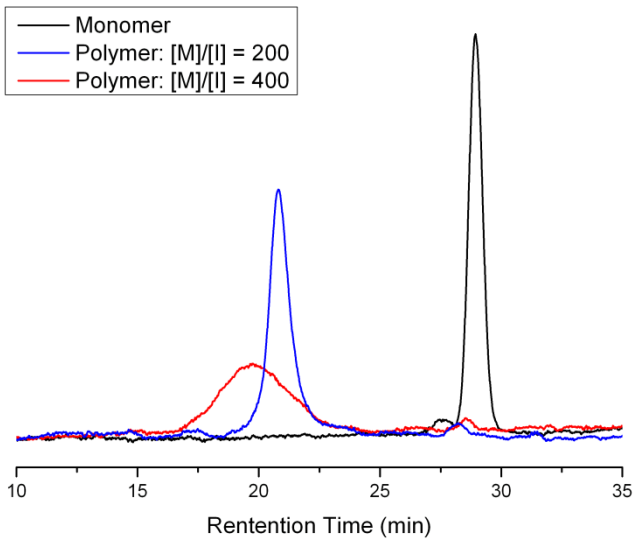

Figure S4: GPC chromatogram of polymer **4d** (with [M]/[I] = 400) and a similar polymer with [M]/[I] =200, compared with the monomer **3d**, recorded using chlorobenzene as the eluent.

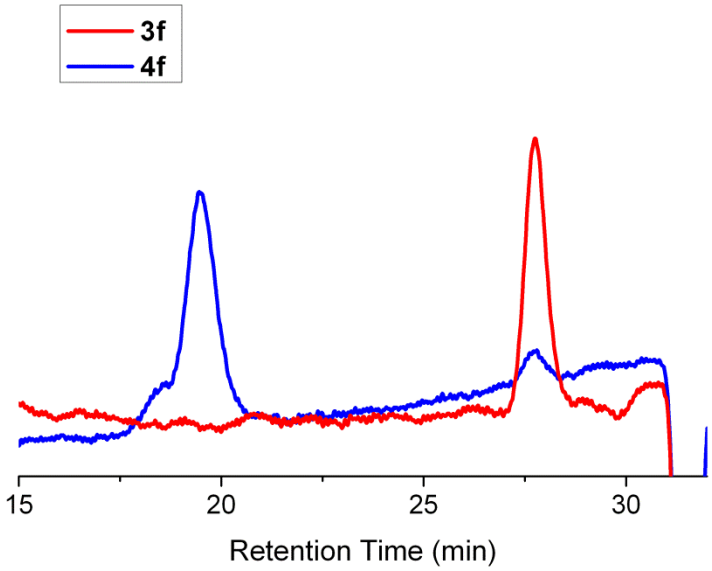

Figure S5: GPC chromatogram of polymer **4f** (with [M]/[I] = 400), compared with the monomer **3f**, recorded using chlorobenzene as the eluent.

5. Thermogravimetric analysis

Thermogravimetric analysis (TGA) was performed on a Mettler Toledo AG - TGA/SDTA851^e model. All the samples were scanned from 25 to 550 °C at a temperature raising rate of 10 °C/min. The C_{60} contents of polymers **4a~d** and **4f** were calculated to be 33.2, 36.6, 37.8, 52.9 and 48.4%, respectively, on the assumption that every single side-chain of the polymer was decorated by a C_{60} unit.

TGA analysis (Figure S6) of these polymers demonstrated that they all undergo a fast weight loss at 290~420 °C, which can be attributed to the decomposition of the polynorbornene main-chain and the polystyrene/alkyl side chains. After passing 420 °C, the samples kept losing weight but at a much slower rate. Considering the fact that C_{60} is

thermally stable under the TGA temperature range (<550 °C), we assume that the materials left over at 550 °C should be mostly fullerene. Indeed, the trend of residual weight of samples **4a~d** and **4f** at 550 °C (43.7, 45.3, 46.1, 66.9, and 53.5% respectively) correlated well with the trend for C_{60} theoretical content of the polymers: the more C_{60} content, the more weight percentage was left over at a higher temperature. The slightly higher weight percentage of the samples at 550 °C on TGA compared to the theoretical fullerene content is probably a result of the residue formed after the polystyrene side chain and the polymer mainchain decomposed at such temperature.

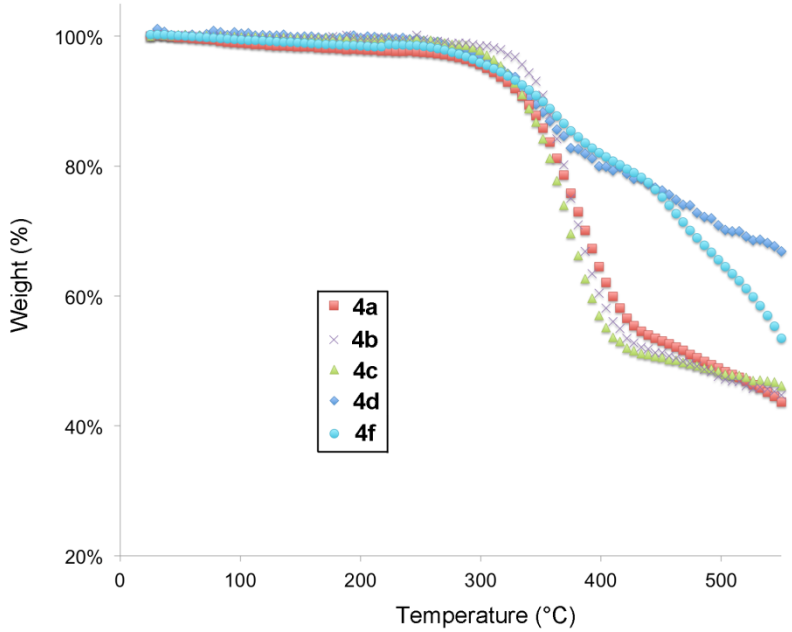

Figure S6: TGA trace of polymers **4a~d** and **4f** from 25 °C to 550 °C.

6. Atomic Force Microscopy

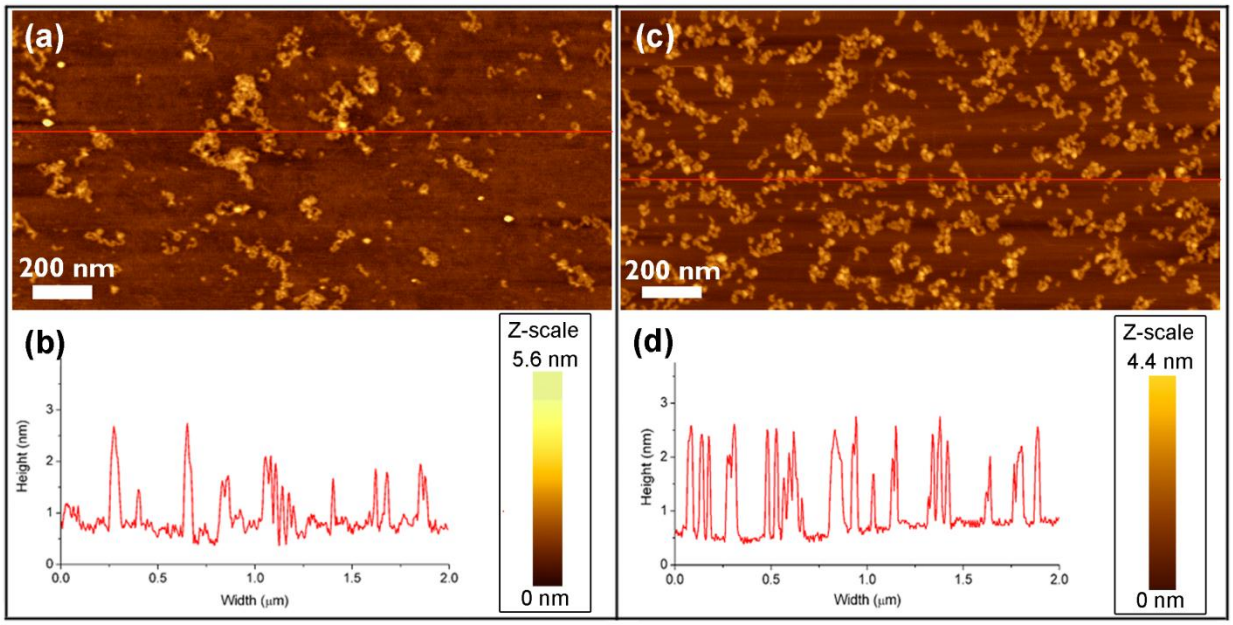

Figure S7. Intermittent contact mode AFM images of polymer **4b** and **4c** spin-cast (5000 rpm) onto mica surface. (a) the height image of **4b**; (b) the profile plot on the red line in (a); (c) the height image of **4c**; (d) the profile plot on the red line in (c). Z-scales are provided next the height profile plots.

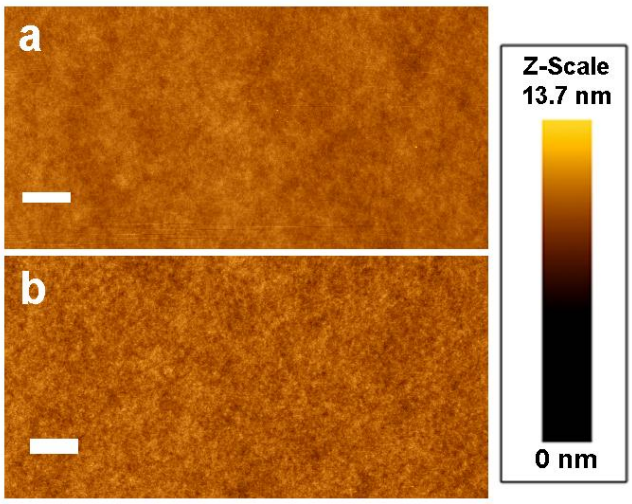

Figure S8. AFM image of the active layer of TFT devices fabricated by **3d** (a) and **4d** (b). The scale bars are 500 nm in length. The average roughness of image (a) was 0.24 nm while that of image b was 0.28 nm. Z-scale to the image is provided next to the figure.

AFM images were taken using intermittent contact mode (light tapping regime) using a Multimode AFM (Veeco). Dilute solution of polymer **4b** and **4c** in *ortho*-dichlorobenzene(0.02 mg/mL) were spin-casted (5000 rpm) onto mica surface. Individual polymer chains can be identified in the corresponding AFM images (Figure S7). The feature heights of the chains were consistently measured to be either ~1 or ~2 nm, representing the height of a single chain and the accumulated height of two or three chains folding onto each other. Although it was difficult to quantify the average contour length of the polymer chains due to their curvy nature, we can clearly identify that >80% of the non-aggregated chains of **4c** were within the range of 200±100 nm. The polymer chains of **4b**, however, were generally much longer because of the higher MW and showed a much broader length distribution due to its higher PDI (2.2) compared to that of **4c** (1.2). In contrast, the single polymer chain features of **4d** were difficult to be observed under the same conditions, as a result of its less visible side-chain 2-decyl-tetradecanyl group compared to the polystyrene group in **4b** and **4c**.

Surface morphology of the thin films of **3d** and **4d** was measured by intermittent contact mode AFM. Both the thin films of the polymer and the monomer were smooth and amorphous. For example, the mean roughness of a thin-film of **4d** was measured by AFM to be 0.28 nm and that of its monomer **3d** was 0.24 nm (Figure S8).

7. Cyclic voltammetry measurement

The cyclic voltammetry measurements on **3d** and **4d** were performed in *o*-DCB solution (1 mg/mL). 0.05 mol/L tetrabutylammonium hexafluorophosphate was used as the

electrolyte. A tiny amount (< 0.1 mg/mL) of ferrocene was added to the solution to serve as the internal reference. The working electrode was glassy carbon (polished), while the reference electrode was Ag/AgCl. The scan rate was set to 50 mV/s.

As shown in the scans, the C_{60} units on the polymer had higher electron affinity compared to that on the monomer. As a result, the calculated LUMO level of the polymer is deeper than that of the monomer. The ~50 mV shift on the reduction potential can be attributed to the aggregated nature of the fullerene units along the polymer chain even in diluted solution. Such phenomenon had been observed in the solid-state before.[24]

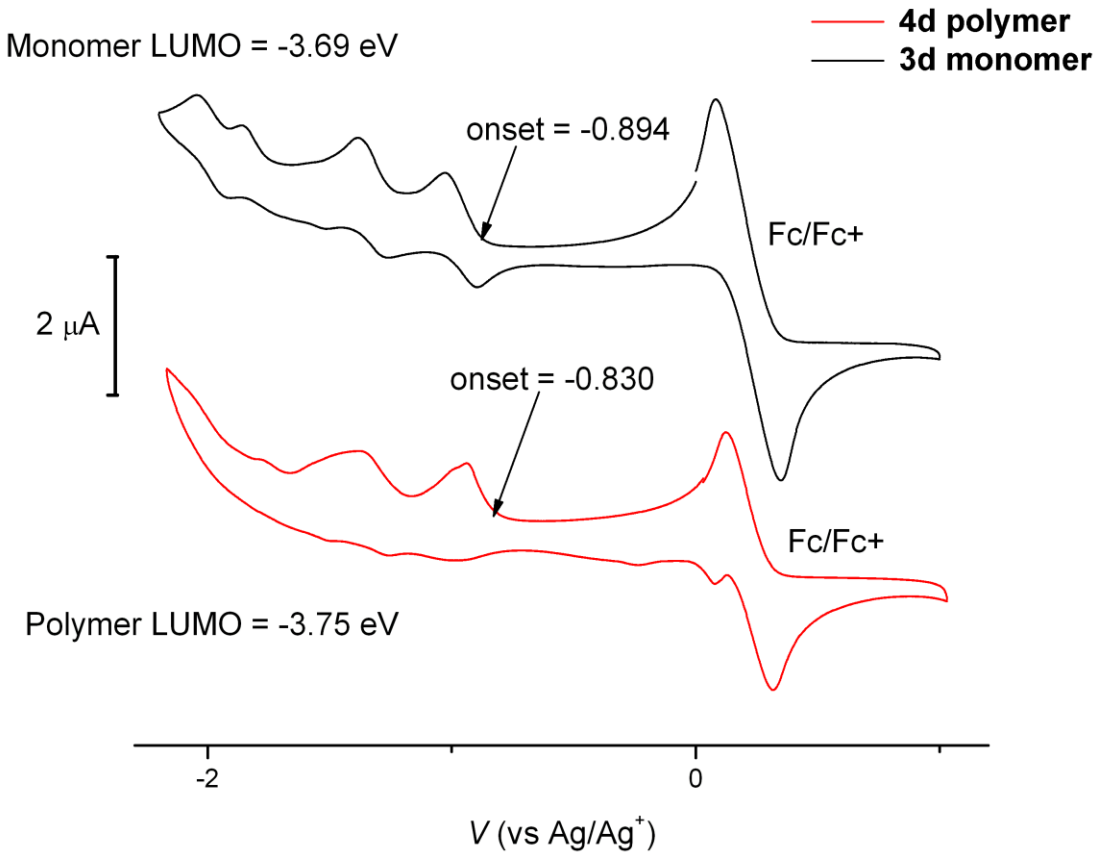

Figure S9. Cyclic voltammetry data of the monomer **3d** (black) and polymer **4d** (red) in *o*-DCB solution (1 mg/mL).

8. Grazing incidence X-ray diffraction

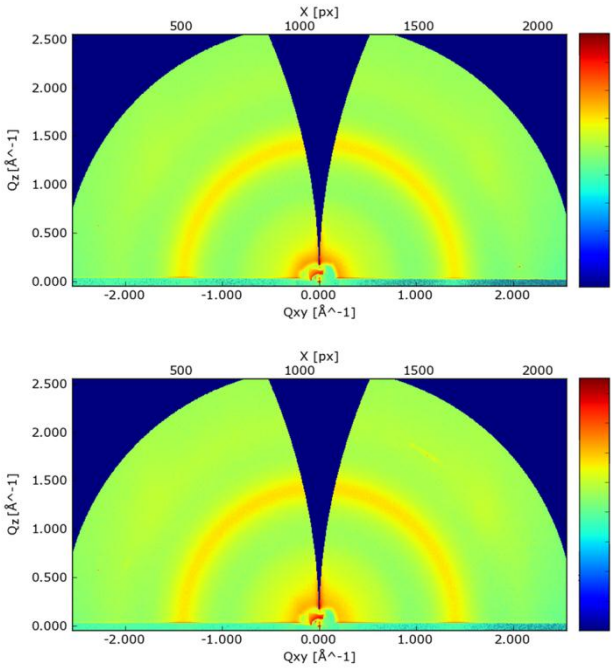

Figure S10. GIXD figures of the thin films of **3d** (top) and **4d** (bottom), recorded on a BCB covered SiO_2 (300 nm)/Si substrate. They demonstrated that both the films are amorphous without any identifiable crystalline domain.

Grazing incidence X-ray diffraction (GIXD) was performed at the Stanford Synchrotron Radiation Lightsource (SSRL) on beamline 11-3. A photon energy of 12.73 keV was used, and the scattering intensity was recorded on a 2-D image plate (MAR-345) with a pixel size of 150 μm (2300 × 2300 pixels), located at a distance of 400 mm from the sample center. The distance between the sample and the detector was calibrated using a LaB_6 polycrystalline standard. The incidence angle was chosen to be 0.14°. The beam size was 50 μm × 150 μm, which resulted in a beam exposure on the sample 150 μm wide over the entire length of the 20 mm sample. The data was distortion corrected (theta-

dependent image distortion introduced by planar detector surface) before performing quantitative analysis on the images. Numerical integration of the diffraction peak areas was performed with the software WxDiff.[25]

9. FET data of polymer 4a~c.

Table S2. Average mobility, On/Off ratio, and Threshold voltage measured in N_2 for the OTFT devices fabricated using **3a~c** and **4a~c**, as well as that measured in air for **4d** before and after soaking the device in toluene for 24 h.

Samples	Mobility (cm^2/Vs)	On/Off	V_t
3a~c	$< 1 \times 10^{-7}$	N/A	N/A
4a	$(3.5 \pm 0.7) \times 10^{-6}$	360	41 ± 10
4b	$(1.8 \pm 0.3) \times 10^{-6}$	180	51 ± 13
4c	$(2.1 \pm 0.6) \times 10^{-6}$	260	65 ± 11
4d in Air	$(8.5 \pm 1.8) \times 10^{-5}$	1000	70 ± 7
4d after soaking in toluene	$(3.8 \pm 1.5) \times 10^{-5}$	900	64 ± 10

The thin film transistors of polymer **4a~c** were fabricated and measured in N_2 under the same conditions as that of **4d**. The electron mobilities, on/off ratio and threshold voltages of these devices are listed in Table S2. The thin films of **4a~c** exerted marginal field effects on account of their low contents of C_{60} and high contents of polystyrene side chains. The polystyerene chains could serve as a thick insulating sheath around the conductive C_{60} core, making the intermolecular charge transport unfavorable. In comparison, the monomers **3a~c** showed marginal field effect (electron mobility $< 1 \times 10^{-7}$ cm^2/Vs) under the similar conditions.

References for SI

1. D. A. Case, T. A. Darden, T. E. Cheatham, C. L. Simmerling, J. Wang, R. E. Duke, R. Luo, M. Crowley, R. C. Walker, W. Zhang, K. M. Merz, B. Wang, S. Hayik, A. Roitberg, G. Seabra, I. Kolossváry, K. F. Wong, F. Paesani, J. Vanicek, X. Wu, S. R. Brozell, T. Steinbrecher, H. Gohlke, L. Yang, C. Tan, J. Mongan, V. Hornak, G. Cui, D. H. Mathews, M. G. Seetin, C. Sagui, V. Babin and P. A. Kollman, *AMBER 11, University of California, San Francisco, 2011*.
2. J. Wang, R. M. Wolf, J. W. Caldwell, P. A. Kollman and D. A. Case, *J. Comput. Chem.*, 2004, **25**, 1157-1174.
3. C. I. Bayly, P. Cieplak, W. Cornell and P. A. Kollman, *J. Phys. Chem.*, 1993, **97**, 10269-10280.
4. B. H. Besler, K. M. Merz and P. A. Kollman, *J. Comput. Chem.*, 1990, **11**, 431-439.
5. U. C. Singh and P. A. Kollman, *J. Comput. Chem.*, 1984, **5**, 129-145.
6. M. J. Frisch, G. W. Trucks, H. B. Schlegel, G. E. Scuseria, M. A. Robb, J. R. Cheeseman, G. Scalmani, V. Barone, B. Mennucci, G. A. Petersson, H. Nakatsuji, M. Caricato, X. Li, H. P. Hratchian, A. F. Izmaylov, J. Bloino, G. Zheng, J. L. Sonnenberg, M. Hada, M. Ehara, K. Toyota, R. Fukuda, J. Hasegawa, M. Ishida, T. Nakajima, Y. Honda, O. Kitao, H. Nakai, T. Vreven, J. A. Montgomery Jr., J. E. Peralta, F. Ogliaro, M. Bearpark, J. J. Heyd, E. Brothers, K. N. Kudin, V. N. Staroverov, R. Kobayashi, J. Normand, K. Raghavachari, A. Rendell, J. C. Burant, S. S. Iyengar, J. Tomasi, M. Cossi, N. Rega, J. M. Millam, M. Klene, J. E. Knox, J. B. Cross, V. Bakken, C. Adamo, J. Jaramillo, R. Gomperts, R. E. Stratmann, O. Yazyev, A. J. Austin, R. Cammi, C. Pomelli, J. W. Ochterski, R. L. Martin, K. Morokuma, V. G. Zakrzewski, G. A. Voth, P. Salvador, J. J. Dannenberg, S. Dapprich, A. D. Daniels, Ö. Farkas, J. B. Foresman, J. V. Ortiz, J. Cioslowski and D. J. Fox, Gaussian, Inc., Pittsburgh, PA, Gaussian 09, Revision A.02 edn., 2009.
7. C. M. Baker and G. H. Grant, *J. Chem. Theory Comput.*, 2007, **3**, 530-548.
8. C. E. A. F. R. Schafmeister, W. F.; Romanovsky, V. University of California, San Francisco, 1995.
9. C. Sagui and T. A. Darden, *Annu. Rev. Biophys. Biomol. Struct.*, 1999, **28**, 155-179.
10. J.-P. Ryckaert, G. Ciccotti and H. J. C. Berendsen, *J. Comput. Phys.*, 1977, **23**, 327-341.
11. X. Wu and B. R. Brooks, *Chem. Phys. Lett.*, 2003, **381**, 512-518.
12. S. Kundu, J. S. Melton, D. C. Sorensen and G. N. Phillips, *Biophys. J.*, 2002, **83**, 723-732.
13. P. Radivojac, Z. Obradovic, D. K. Smith, G. Zhu, S. Vucetic, C. J. Brown, J. D. Lawson and A. K. Dunker, *Protein Science*, 2004, **13**, 71-80.
14. K. Senthilkumar, F. C. Grozema, F. M. Bickelhaupt and L. D. A. Siebbeles, *J. Chem. Phys.*, 2003, **119**, 9809-9817.
15. J. E. Norton and J.-L. Brédas, *J. Chem. Phys.*, 2008, **128**, 034701.
16. A. D. Becke, *J. Chem. Phys.*, 1993, **98**, 5648-5652.
17. C. T. Lee, W. T. Yang and R. G. Parr, *Phys. Rev. B*, 1988, **37**, 785-789.

18. M. M. Francl, W. J. Pietro, W. J. Hehre, J. S. Binkley, M. S. Gordon, D. J. Defrees and J. A. Pople, *J. Chem. Phys.*, 1982, **77**, 3654-3665.
19. P. C. Harihara and J. A. Pople, *Theor. Chem. Acc.*, 1973, **28**, 213-222.
20. W. J. Hehre, R. Ditchfie and J. A. Pople, *J. Chem. Phys.*, 1972, **56**, 2257-2261.
21. Y. Shao, L. F. Molnar, Y. Jung, J. Kussmann, C. Ochsenfeld, S. T. Brown, A. T. B. Gilbert, L. V. Slipchenko, S. V. Levchenko, D. P. O'Neill, R. A. DiStasio Jr, R. C. Lochan, T. Wang, G. J. O. Beran, N. A. Besley, J. M. Herbert, C. Yeh Lin, T. Van Voorhis, S. Hung Chien, A. Sodt, R. P. Steele, V. A. Rassolov, P. E. Maslen, P. P. Korambath, R. D. Adamson, B. Austin, J. Baker, E. F. C. Byrd, H. Dachsel, R. J. Doerksen, A. Dreuw, B. D. Dunietz, A. D. Dutoi, T. R. Furlani, S. R. Gwaltney, A. Heyden, S. Hirata, C.-P. Hsu, G. Kedziora, R. Z. Khalliulin, P. Klunzinger, A. M. Lee, M. S. Lee, W. Liang, I. Lotan, N. Nair, B. Peters, E. I. Proynov, P. A. Pieniazek, Y. Min Rhee, J. Ritchie, E. Rosta, C. David Sherrill, A. C. Simmonett, J. E. Subotnik, H. Lee Woodcock Iii, W. Zhang, A. T. Bell, A. K. Chakraborty, D. M. Chipman, F. J. Keil, A. Warshel, W. J. Hehre, H. F. Schaefer Iii, J. Kong, A. I. Krylov, P. M. W. Gill and M. Head-Gordon, *Phys. Chem. Chem. Phys.*, 2006, **8**, 3172-3191.
22. J. Kirkpatrick, 2007, PhD Dissertation, University of London.
23. J. Huang and M. Kertesz, *Chem. Phys. Lett.*, 2004, **390**, 110-115.
24. F. C. Jamieson, E. B. Domingo, T. McCarthy-Ward, M. Heeney, N. Stingelin and J. R. Durrant, *Chemical Science*, 2012, **3**, 485-492.
25. S. C. B. Mannsfeld, M. L. Tang and Z. A. Bao, *Adv. Mater.*, 2011, **23**, 127-131.